

Occurrence and distribution of invisible gold in a Carlin-type gold deposit in China

SHUI HE MAO

Institute of Comprehensive Utilization of Mineral Resources, Emei, Sichuan 614200, People's Republic of China

ABSTRACT

From the results of EPMA on various minerals from the ore and from SEM observations and chemical dissolution experiments on pyrite in a Carlin-type gold deposit (Banqi gold deposit, Guizhou, China), the following conclusions are drawn:

Pyrite is the most important Au-bearing mineral. Most of the pyrite grains occur as anhedral granules consisting of earlier formed, euhedral crystal cores containing little or no Au and As and later formed rims that are rich in Au and As. The average tenor of Au is 257.6 ppm in pyrite, about 600 ppm in rims of anhedral grains, and less than 82 ppm in cores.

There is a positive correlation between the concentrations of Au and As, so the distribution of Au is similar to that of As in SEM images and EPMA data.

EPMA data show highly variable Au concentrations at different spots in a Au-rich rim within a pyrite grain. Moreover, in chemical dissolution tests on pyrite, most of the Au is not in the supernatant HNO₃ solution but remains in the undissolved residues and is available for leaching into KI + I₂ Au-leaching solution. All these facts illustrate that Au in pyrite occurs as ultramicroscopic native gold inclusions, not as isomorphous substitution.

It is shown that more than 60% of the Au given by chemical assay of clay minerals occurs in submicrometer-size pyrite inclusions in which Au is remarkably enriched.

The Au contents in other minerals, such as arsenopyrite, quartz, calcite, or barite, are all below the detection limit of EPMA. Considering the results of chemical assays of these mineral separates, it is concluded that these minerals are not significantly Au bearing.

Knowledge of the mode of occurrence and distribution characteristics of invisible Au in Carlin-type deposits is beneficial to metallurgical process design for Au recovery. In this case, sufficient oxidation and leaching of the pyrite surface layer will produce satisfactory recovery at reduced cost in time, energy, and reagents.

INTRODUCTION

There is a type of Au-bearing ore in which the Au tenor is quite high—sometimes reaching tens of ppm—but the Au in the ore is not visible by reflected and transmitted light microscopy at high magnification. Generally, this Au is called invisible Au, ultramicroscopic Au, or submicrometer Au.

Because ultramicroscopic Au is invisible, it is extremely difficult to study its occurrence and distribution by conventional determinative means. Spending a great deal of time, the mineralogist can assay hand-picked mineral separates to obtain the average content of Au in each mineral. However, such analyses of mineral separates convey no information as to whether the Au is homogeneously distributed within and among the mineral crystals, is in solid solution, or is present as submicroscopic inclusions.

Assumptions and inferences have been made about the manner of occurrence of invisible Au (Boyle, 1979; Zhang et al., 1987; Cabri et al., 1989; Bakken et al., 1989; Cook and Chrystoulis 1990). However, there is some controversy about whether the Au is present in chemical com-

bination in sulfide minerals such as pyrite and arsenopyrite (i.e., structurally incorporated Au) or whether the Au occurs as submicroscopic inclusions. But none of the studies provides direct and convincing evidence to confirm the inferences. Using an electron-probe microanalyzer (EPMA) and a scanning electron microscope (SEM), the author has investigated the distribution characteristics and concentration of invisible Au at different spots in Au-bearing minerals of various grain sizes, crystal forms, and paragenetic stages. Furthermore, the distribution of invisible Au is displayed by the distribution of As, which is positively correlated with Au in pyrite. Therefore, the present research work has provided a scientific basis for selecting an economical and effective treatment and extraction process for the ore from Banqi gold deposit, Guizhou, a Carlin-type gold deposit in China.

SAMPLE PREPARATION

The unoxidized (primary) ore sample consists of drill cuttings from many parts in the Banqi deposit, which is an epithermal disseminated gold deposit in China. The tectonic position of the Banqi gold deposit is in the syn-

taxis zone of the Youjing late Palaeozoic era–Triassic rift graben and late Precambrian Yangzi platform. The mineralization district emerges in Devonian–Triassic strata; in particular, the mineralized horizons are in the lower Triassic Ziyun formation. The ore bodies are multiply controlled by the vertical main fault of the anticline and arch districts, the fracture zones between the horizons, and the rock characteristics. The most rock is tectonite consisting of clastic rocks of terrigenous sedimentation that are enriched in clayey, silty, and organic materials and sulfides.

The total ore sample weighs 2438 g. Ore blocks were selected for preparing the polished sections and thin sections that were used for mineralogical studies by optical microscopy and for SEM observation and EPMA investigations. The rest of the sample was crushed and then ground to –100 mesh; then a portion was further ground to –200 mesh for Au assay and chemical analyses of S, Fe, Al, and K. Most of the sample of –100 mesh was used to prepare two pyrite concentrates (one >0.074 mm, the other <0.074 mm) by sieving and panning, then removing impurities such as barite by use of a dielectric separator and by hand selecting under a microscope. This produced pure pyrite mineral separates for Au assay and chemical dissolution experiments.

The clay mineral separate with grain size <10 μm and total mass 860 mg was prepared using the pulverized ore sample and a precipitation method. The grain size was estimated according to the precipitation speed and not accurately measured.

EXPERIMENTAL METHODS

Optical microscopy

Mineralogical composition of the ore was obtained by examining quite a number of polished sections and thin sections with reflected and transmitted light microscopy. Modal analysis and the statistics of size distribution of pyrite were determined by point counting. Crystal forms and zoning characteristics of pyrite were investigated by optical microscopy.

EPMA and SEM analyses

The analyses of pyrite, As-bearing pyrite, and other minerals were performed on a JEOL 733 electron probe equipped with a TN 5500 energy-dispersive spectrometer (EDS) system and TN 5600 automation system. The instrument was operated at 25 kV (accelerating voltage) with beam current (cup reading) 20 nA and beam diameter about 1 μm , using the following X-ray lines and standards: AuL α (metal), FeK α and SK α (pyrite), AsL α (arsenopyrite). Fe, S, and As can be measured by EDS with routine procedure; the trace element Au can only be measured by wavelength-dispersive spectrometry (WDS) using special procedures and precautions. The common method for measuring background is to move the spectrometer to both sides of the peak position and measure the count rates, but in detecting trace elements this method is not suitable. In the present work, a pure pyrite crys-

tal free of Au was employed as a standard for measuring background. The background count rate was measured at the AuL α peak position on the blank pyrite standard. One wavelength-dispersive spectrometer with a LiF crystal was dedicated to determine the Au concentration, so that during the entire procedure the spectrometer was not moved from the AuL α position. To reduce the detection limit and the counting statistics error, the counting time for detecting the trace Au was set at 100 s. Under the above conditions, the precision for detecting trace Au in pyrite was improved. The same method for background measurement was used to measure the Au concentrations in arsenopyrite, quartz, calcite, barite, etc. The TASK program provided by Tracor Northern is capable of doing EDS and WDS measurements simultaneously and then performing the quantitative corrections for atomic number, absorption, and fluorescence effects with the ZAF program included in TASK. If AuM α were chosen as the analyzed line and PET as the diffraction crystal, there would be the advantage of lower background count rate and therefore better sensitivity. Unfortunately, there is some overlap between AuM α (5.840 \AA) and the third order line of FeK α (5.812 \AA). Therefore, AuL α is preferable as the analyzed line.

There are several expressions for calculating the detection limit (C_{DL}) by EPMA (Toya and Kato, 1983; Cox, 1983; Ziebold, 1967). In routine work, expression 1 is employed to calculate C_{DL} for a given element:

$$C_{\text{DL}} = \frac{3\sqrt{I_{\text{B}}t}}{(I_{\text{P}} - I_{\text{B}})t} = \frac{3\sqrt{I_{\text{B}}}}{(I_{\text{P}} - I_{\text{B}})\sqrt{t}} \quad (1)$$

where I_{P} is the peak count rate, I_{B} is the background count rate both in counts per second (cps), and t is the counting time. Under the operating conditions mentioned above, I_{P} for Au is approximately 8900 cps, I_{B} is approximately 73 cps, t is 100 s, and the calculated value of C_{DL} by expression 1 is 0.029%. Considering uncertainties such as instrumental instability or sample polish imperfections, the practical C_{DL} value for detecting trace Au in pyrite is estimated to be 0.05%. Therefore, a Au concentration less than 0.05% in any analyzed spot is considered to be zero. If the invisible Au in pyrite is distributed homogeneously, it is almost impossible to be detected by EPMA under the operating conditions employed in this study. However, when the Au is relatively enriched in some areas within pyrite, it becomes possible to investigate the variation and enrichment characteristics of the invisible Au and the relationship between Au and other elements.

Chemical dissolution experiments

Chemical dissolution experiments on pyrite were carried out according to the flow chart shown in Figure 1 using a pyrite sample with the grain size <0.074 mm and total mass 400 mg. Au in solutions and in residue were concentrated by fire assay, then analyzed by atomic absorption spectrometry (AAS). Fe was analyzed by wet chemistry. In the experiments, pyrite is dissolved in HNO₃,

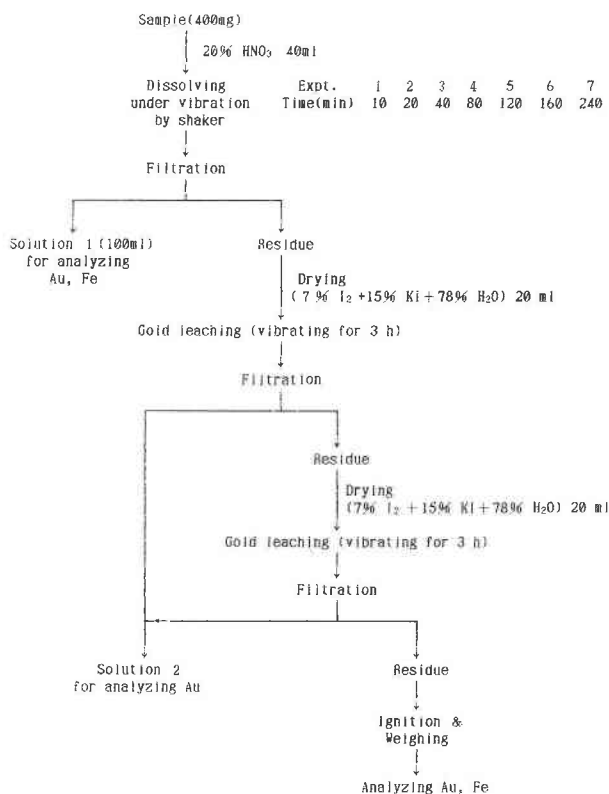


Fig. 1. Flow chart of dissolution experiment on pyrite.

but particulate Au remains insoluble. The addition of a KI + I₂ solution can leach Au from the residue.

RESULTS

Mineralogical and chemical composition of the ore

Fire assay analysis yielded 31.02 ppm Au, and chemical analyses yielded 2.40% S, 3.41% Fe, 2.59% Al, and 1.63% K in bulk ore. The mineralogical study by optical microscopy showed that the sulfides in the ore sample are pyrite, arsenopyrite, marcasite, stibnite, pyrrhotite, chalcopyrite, realgar, orpiment, and pentlandite. The other common minerals present are quartz, illite, kaolinite, calcite, dolomite, apatite, and barite. Modal analysis and point-counting statistics gave 4.7% pyrite (including small

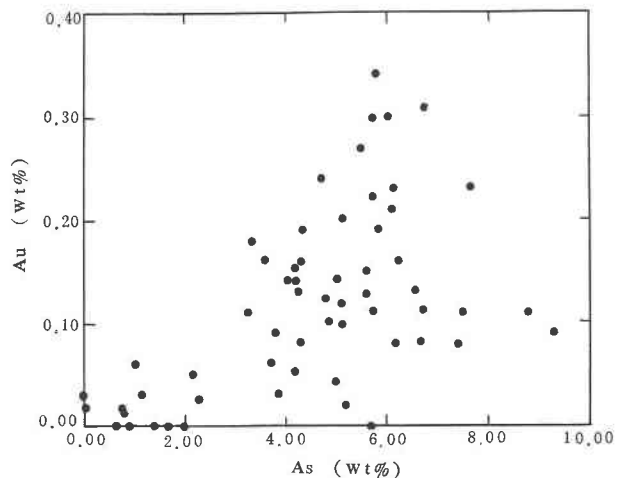


Fig. 2. Correlation between Au and As concentrations in tiny pyrite grains (<10 μm).

quantity of some other sulfides), 68.7% quartz and some carbonates, 26.6% clay minerals.

The pyrite occurs as euhedral crystals and as anhedral granules. The size distribution of pyrite is as follows: pyrite <0.074 mm, 87.40%; pyrite >0.074 mm, 12.60%. More than 95% of the pyrite grains larger than 10 μm occur as anhedral granules; only 5% of these are euhedral and subhedral crystals. The concentrations of Au in different size fractions of pyrite in the ore differ considerably. According to the fire assay results, the Au concentration in pyrite <0.074 mm averages 275.0 ppm, whereas that in pyrite >0.074 mm is 137.1 ppm. Therefore, the pyrite averages 257.6 ppm Au.

Occurrence and distribution of Au in pyrite determined by EPMA and SEM in pyrite grains <10 μm

One hundred and twenty small pyrite grains (<10 μm) from multiple samples were selected for Au analysis by EPMA. In 28 grains the Au concentrations are below the detection limit (0.05%) and As concentrations are in the range 0–5.64% (average 2.05%). In the other 92 grains the Au concentrations are higher than the detection limit, ranging from 0.05% to 0.34% (average 0.15%); As concentrations range from 1.60% to 9.29% (average 5.22%) (Table 1). Figure 2 shows the positive correlation between Au and As concentrations.

TABLE 1. Concentrations of Au and As in minerals analyzed by EPMA

Ana. sp.	sp.	Spots with Au conc. (>0.05%)				Spots with Au conc. (<0.05%)			
		Au (%)		As (%)		As (%)			
		Range	Ave.	Range	Ave.	sp.	Range	Ave.	
Py. (<10 μm)	120	92	0.05–0.34	0.15	1.60–9.29	5.22	28	0–5.65	2.05
Int. of py.*	73	10	0.05–0.11	0.08	0–9.13	2.67	63	0–3.77	0.81
Rims of anh. py.*	57	44	0.05–0.46	0.18	0.85–7.37	5.61	13	0–4.51	0.76
Rims of euh. py.*	18	0					18	0–0.49	0.12

Note: Ana. = Analyzed, anh. = anhedral, Ave. = Average, conc. = concentration, euh. = euhedral, Int. = Interiors, Py. = Pyrite, Sp. = Spots.
* Pyrite grains >10 μm.

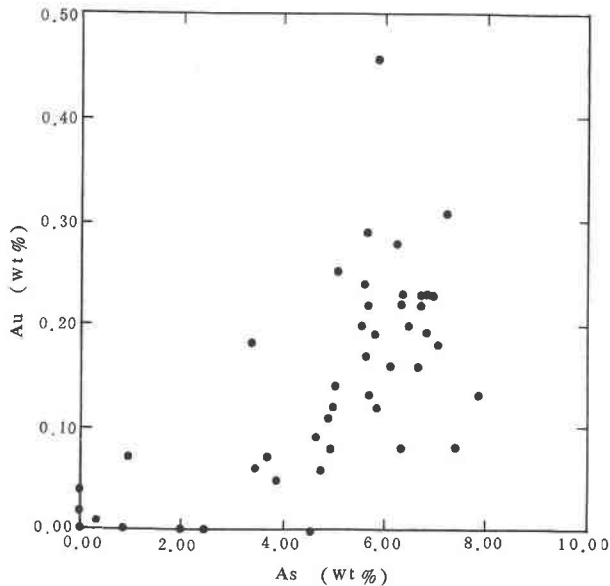


Fig. 3. Correlation between the Au and As concentrations in rims of anhedral pyrite grains $> 10 \mu\text{m}$.

Interior of the pyrite grains $> 10 \mu\text{m}$

Randomly chosen pyrite grains within the range of $10 \mu\text{m}$ to about $100 \mu\text{m}$, with different crystal forms in a number of polished sections, were analyzed. Several spots were analyzed in each grain, yielding 73 spots in total. Among them, 63 spots had Au concentrations $< 0.05\%$ and As concentrations ranging between zero and 3.77% (average 0.81%). Only in ten spots are the Au concentrations higher than the detection limit, ranging from 0.05% to 0.11% (average 0.08%); in the ten, As concentrations range between zero and 9.13% (average 2.67%) (see Table 1).

In rims of pyrite grains $> 10 \mu\text{m}$

The concentrations of Au and As in the rims of euhedral pyrite grains are quite distinct from rims of anhedral pyrite grains. Data on Au and As concentrations in 18 spots located near the edges of several euhedral pyrite grains are shown in Table 1. Au concentrations are everywhere below the detection limit, and As concentrations range between zero and 0.49% (average 0.12%).

Fifty-seven spots were analyzed in a number of anhedral pyrite grains. In 13 spots, the Au concentrations are below the detection limit, and the As concentrations range from zero to 4.51% (average 0.76%). In the other 44 spots, the Au concentrations are higher than the detection limit, ranging from 0.05% to 0.46% (average 0.18%), and the As concentrations range from 0.85% to 7.37% (average 5.61%) (Table 1). Figure 3 shows the positive correlation between the concentrations of Au and As. The particular relation between the concentrations of Au and As indicates that the distribution of trace Au can be displayed qualitatively using the X-ray images of As in pyrite grains.

X-ray images in Figures 4 and 5 that were produced

by electron beam scanning clearly show that As is conspicuously enriched in the rims of pyrite grains, and little or no As is contained in the interior of pyrite grains. Therefore, according to the positive correlation between the concentrations of Au and As, it is believed that Au must be enriched in the rims of pyrite grains. The secondary electron images (SEI) in Figures 4 and 5 show that there are boundary lines between the rims and interiors of pyrite grains. This indicates that anhedral pyrite grains in this gold deposit consist of earlier formed, euhedral crystal cores containing little Au and As and later formed rims containing remarkably rich Au and As, i.e., with a distinct zoning texture.

Au concentrations in arsenopyrite and other minerals determined by EPMA

Arsenopyrite. Au concentrations have been determined in 22 spots that are located at rims and interiors of arsenopyrite grains of different shapes and sizes, selected in several polished sections. Except one spot with a Au concentration equal to 0.15% , the Au concentrations are below the detection limit. In addition, the arsenopyrite is very sparsely disseminated in the ore.

Quartz. Within tens of quartz grains with different sizes, 59 spots were selected in different areas for Au analysis. In five spots the Au concentrations are just above the detection limit: 0.06 , 0.05 , 0.09 , 0.07 , 0.08% ; the Au concentrations in the other 54 spots are below detection limit. Additionally, chemical assay shows that the average Au concentration in quartz is 0.08 ppm (Song and Diao, 1989).

Calcite. In 40 analyzed spots, only two have Au concentrations just above detection limit, 0.06% and 0.05% . The Au concentrations in the other 38 spots are below the detection limit. The chemical assay indicates that the Au concentration in carbonates averages 0.08 ppm (Song and Diao, 1989).

Barite. One spot had a Au concentration just at the detection limit (0.05%); Au concentrations are otherwise below the detection limit.

On the basis of the above results, it can be concluded that arsenopyrite, quartz, calcite, and barite are not significant Au-bearing minerals.

Clay minerals. The clay minerals are illite and kaolinite. Among 70 randomly selected spots in clay minerals, Au concentrations detected by EPMA are well above the detection limit in some spots. However, the EDS spectra of the corresponding spots show small peaks of S, As, and Fe, indicating that there may exist some very fine, As-bearing pyrite inclusions in the clay mixture. This inference is confirmed by the electron-beam scanning images for clay minerals. To determine whether the Au detected in some spots of clay by EPMA is contained in the clay mineral itself or in the micropyrroite inclusions, the clay mineral separate with grain size $< 10 \mu\text{m}$ was prepared for chemical analysis of the concentrations of Au and S, and then the content of pyrite was calculated from

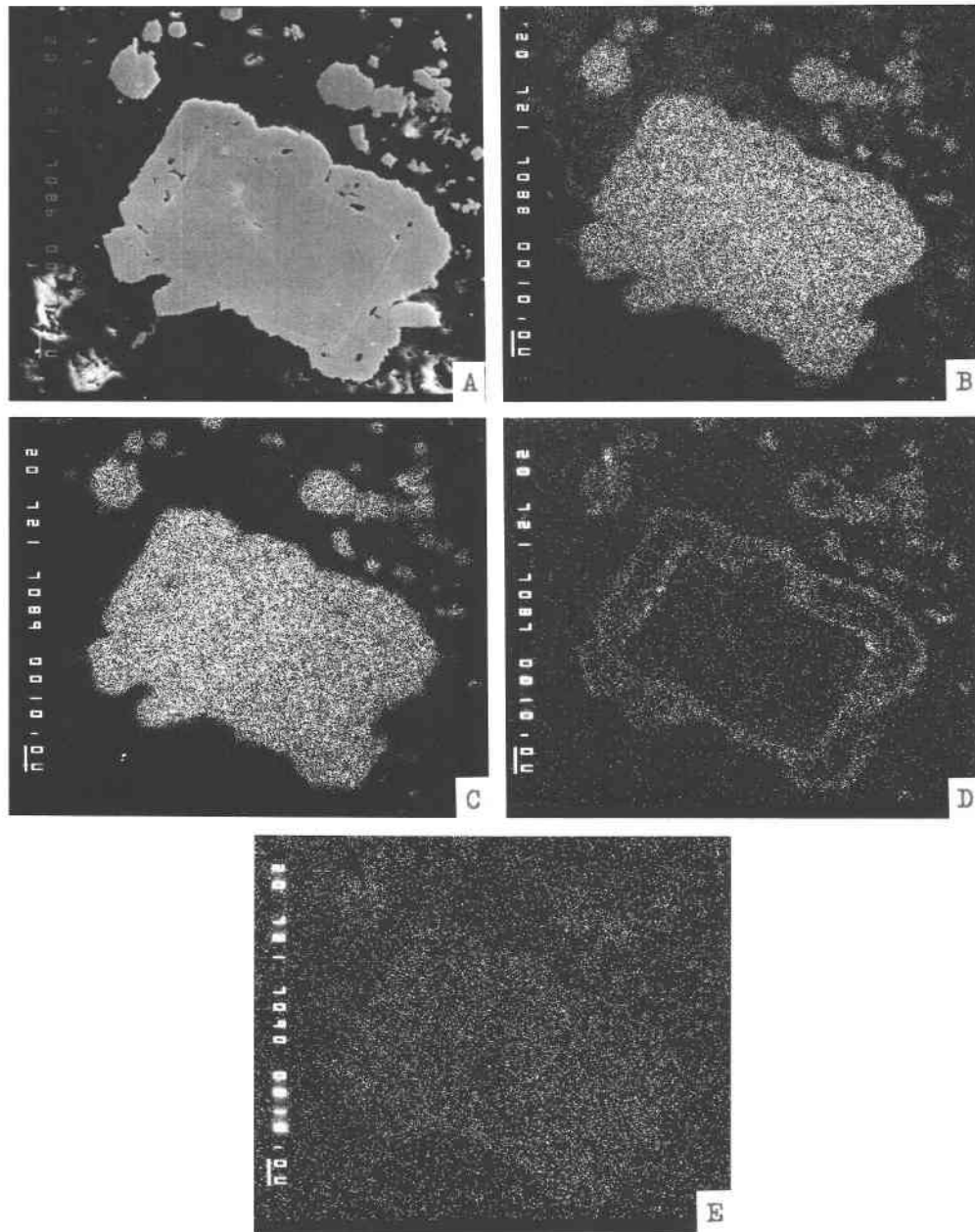


Fig. 4. Electron-beam scanning images on an anhedral pyrite grain. (A) SEI, (B) $FeK\alpha$, (C) $SK\alpha$, (D) $AsL\alpha$, (E) $AuL\alpha$.

the S concentration. Au assay of 860 mg of clay mineral separate of grain size $<10\ \mu\text{m}$ yielded 33.24 ppm Au and 1.75 wt% S, which can be recalculated as 3.27% pyrite as microscopic inclusions identified by SEM. The average Au concentration in clay minerals is far below the detection limit of EPMA, so it is believed that the Au detected in some spots of clay minerals is actually or mostly contained in micrometer-size pyrite inclusions that are remarkably enriched with Au. Another question of interest is what percentage of the Au content given by clay assays

occurs in micropyrrite inclusions vs. in the clay mineral structures. It is reasonable to consider that the Au concentration in micropyrrite inclusions is probably at least equal to that in rims of the anhedral pyrite grains, i.e., 600 ppm or more (see below). Combining this with assay data of the clay mineral separate, we can make a rough calculation: the Au quantity contained in a 1-g clay sample is 33.24 μg , the quantity of pyrite inclusions is 0.0327 g, and these contain about 19.6 μg of Au at the 600 ppm level. Therefore, it is reasonably certain that about 60%

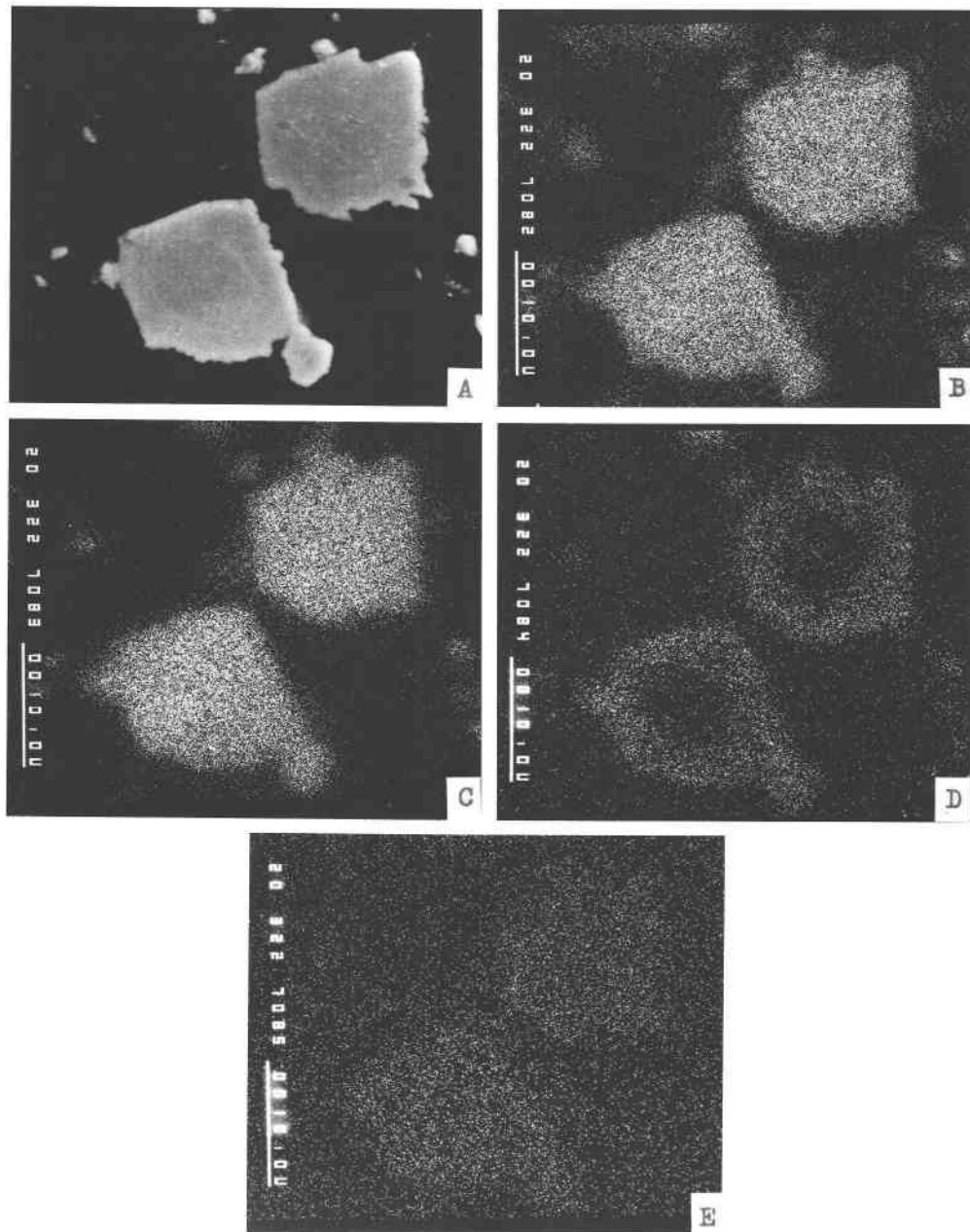


Fig. 5. Electron-beam scanning images on an anhedral pyrite grain. (A) SEI, (B) FeK α , (C) SK α , (D) AsL α , (E) AuL α .

or more of the Au in clay mineral assays occurs in the micropyrrite inclusions.

Results of chemical dissolution experiments

To confirm the conjecture drawn from the EPMA and SEM results, chemical dissolution experiments on pyrite have been carried out, and a series of very meaningful results were obtained (Table 2). Using the data from Table 2, the correlations between the leaching time by HNO₃ and the Au concentrations both in solutions and in residue are shown in Figure 6. The correlations between the

leaching time by HNO₃ and the Au concentrations both in dissolved pyrite and in undissolved pyrite remaining in the residue are shown in Figure 7.

In experiments lasting 10, 20, and 40 min, the Au concentrations in HNO₃ solution increase approximately linearly with time, so the solution is undersaturated with Au. There appears to be a large excess of NO₃⁻ ion relative to dissolved S species, so complete oxidation of dissolved S seems likely. In this case, the Au solubility would not be affected by formation of complexes with polysulfide, thiosulfate, sulfite, or other incompletely oxidized S an-

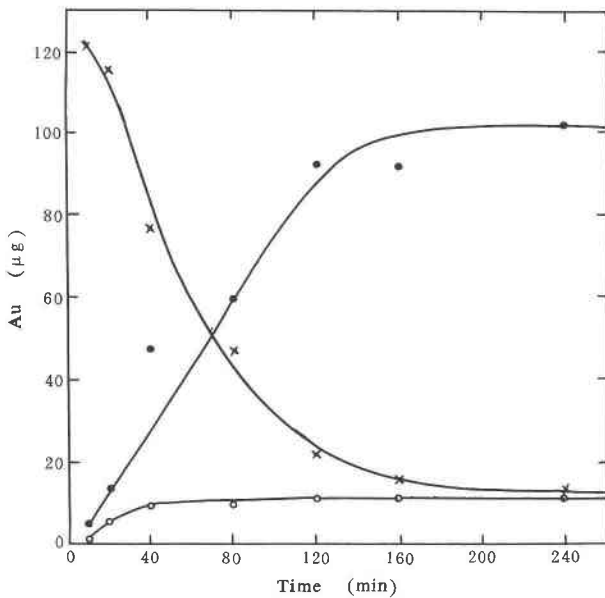


Fig. 6. Correlation between dissolution time (min) by HNO_3 and the Au contents (μg) in solutions and in residue. Open circles are in HNO_3 solution, solid circles in $\text{KI} + \text{I}_2$ solution, crosses in residue.

ions that might enhance the solubility of crystalline Au as more pyrite dissolves in longer experiments (Webster, 1986). Therefore, the first three experiments did not precipitate Au that was liberated from pyrite during the dissolution of pyrite. On the other hand, the Au that was liberated from the dissolved pyrite and was not present in the HNO_3 solution was dissolved subsequently upon the addition of $\text{I}_2 + \text{KI}$. This must represent Au that occurred in pyrite as discrete metal particles, not as crystalline Au. Therefore, it is reasonable to conclude that most of the Au contained in pyrite occurs as ultramicroscopic particulate native gold inclusions.

The Au concentration in the $\text{KI} + \text{I}_2$ solution increases dramatically with dissolution time up to 120 min, then increases very slowly (Fig. 6). After 160 min, the Au concentration reaches a plateau even though more pyrite is continuously dissolved by HNO_3 , and the Fe concentra-

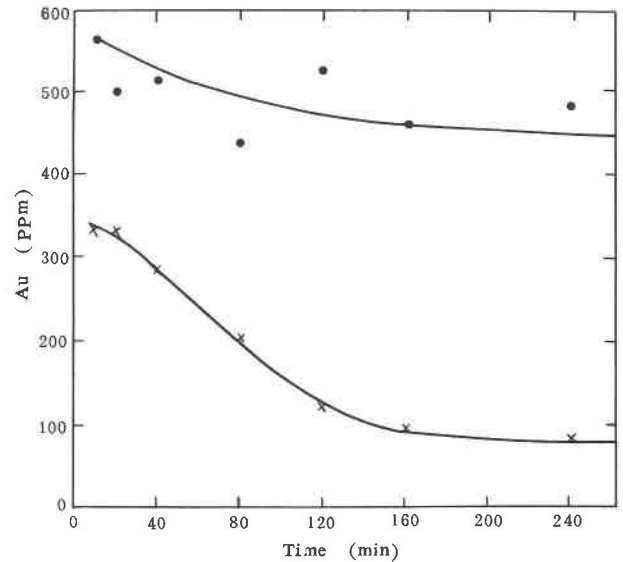


Fig. 7. Correlation between dissolution time (min) by HNO_3 and the Au concentrations (ppm) both in dissolved pyrite and in undissolved pyrite remaining in residue. Solid circles are in dissolved pyrite, crosses in undissolved pyrite.

tion in HNO_3 solution increases up to 240 min. This suggests that in the period between 160 and 240 min the Au concentrated in pyrite rims has been dissolved out.

The concentration of Au in the residue decreases sharply over the interval between 10 and 120 min, and then it gradually slows down. After 160 min, little variation of Au concentration is detected in the residue. This result is in good agreement with the above description, i.e., the upper curve in Figure 6 and lower curve in Figure 7 are mirror images.

It is likely that when the dissolution time is less than 120 min, the dissolution is of pyrite rims in which Au is enriched. However, there is a wide range of size distribution for pyrite grains and of thickness for pyrite rims. It is likely that the rims of pyrite grains with smaller size and thinner rims have already been dissolved out in less than 120 min. Therefore, it is reasonable to assume that the Au concentration in pyrite dissolved by HNO_3 in 10

TABLE 2. Results of chemical dissolution experiments on pyrite

No.	Disso. time (min)	Au cont. (μg)				Fe conc. in HNO_3 Sol. 1 (mg/mL)	Py. quan. in HNO_3 Sol. 1 (mg)	Resi. quan. (mg)	Fe cont. in resi. (%)	Py. quan. in resi. (mg)	Au conc. in dissd. Py. by HNO_3 (ppm)	Au conc. in undiss. Py. (ppm)
		HNO_3 Sol. 1 (100 mL)	$\text{KI} + \text{I}_2$ Sol. 2	Resi.	Total							
1	10	0.95	5.17	121.26	127.38	0.05	10.74	329.5	51.02	361.12	569.8	335.8
2	20	5.79	13.72	115.74	135.25	0.18	38.67	319.0	50.65	347.15	504.5	333.4
3	40	9.36	48.38	77.22	134.96	0.52	111.71	265.0	47.26	268.96	516.9	287.1
4	80	9.83	60.50	47.11	117.44	0.74	158.97	227.8	47.44	232.22	442.4	202.9
5	120	11.04	92.76	24.01	127.31	0.91	195.49	200.3	45.34	195.06	531.0	123.1
6	160	11.28	92.28	15.86	119.42	1.04	223.42	180.5	44.84	173.79	463.5	91.3
7	240	12.34	102.00	12.70	127.04	1.09	234.16	167.5	43.08	155.10	488.3	81.9

Note: Disso. = Dissolving, Sol. = solution, cont. = content, Resi. = Residue, conc. = concentration, Py = Pyrite, quan. = quantity, undiss. = undissolved, dissd. = dissolved.

min was that in pyrite rims, i.e., 569.8 ppm (Table 2). In addition, microscopic observation shows that about 5% of the pyrite grains prepared for the dissolution experiment occur as euhedral crystals, which have been proved to contain little or no Au, so the Au concentration in rims of anhedral pyrite grains should be near 600 ppm.

It is apparent that the Au concentration in the interior of pyrite (euhedral core of anhedral pyrite grain) is approximately equal to or less than that in the pyrite residue after dissolving for 240 min, i.e., 82 ppm.

DISCUSSION AND CONCLUSIONS

Of the various minerals in the ore, pyrite is clearly the most important Au-bearing mineral. More than 95% of the pyrite grains occur as anhedral granules that consist of an earlier formed, euhedral crystal core containing little Au and As and later formed rims notably enriched in Au and As. There is little or no Au in euhedral pyrite crystals. The average Au concentration in pyrite is 257.6 ppm. The average Au concentration in the rims of anhedral pyrite grains is about 600 ppm, whereas the interior of the grains contains less than 82 ppm.

Usually there is no way of observing and displaying the invisible Au in pyrite grains because of its trace content (see Figs. 4E and 5E). The distribution characteristic of invisible Au in pyrite can however be displayed and examined by imaging arsenic by SEM because of the positive correlation between the concentrations of Au and As.

In chemical dissolution experiments on pyrite, the Au liberated from dissolved pyrite does not enter into HNO₃ solution but resides in the residue together with the undissolved pyrite. The Au in the residue can be dissolved by the Au-leaching solution. In addition, EPMA data indicate that Au concentrations at different points in the Au-rich rims of pyrite grains are remarkably different. It is confirmed from these facts that the invisible Au in pyrite occurs as ultramicroscopic native gold inclusions, not as isomorphous substitution.

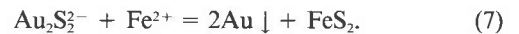
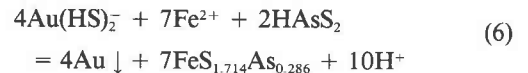
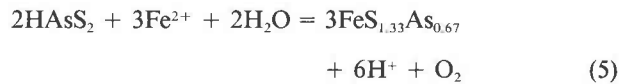
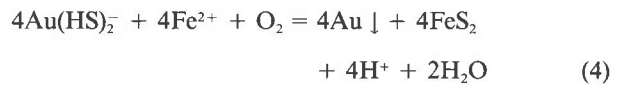
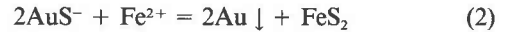
The Au concentrations in other minerals, such as arsenopyrite, quartz, calcite, or barite, are nearly all below the detection limit of EPMA (0.05%). In association with the results of chemical assays of mineral separates, it is clear that these minerals are not substantially auriferous.

More than 60% of the Au content given by chemical assay of clay minerals occurs in submicrometer-scale pyrite inclusions in which Au is remarkably enriched.

The ore in the Banqi gold deposit is very similar to that from the Carlin and Cortez gold mines, Nevada, U.S.A., in the following aspects: the manner of occurrence and distribution characteristics of the invisible Au, the positive correlation between Au and As concentrations, the microstructure of the main Au-bearing minerals, and the mineralogical composition of the ore. This indicates that the Carlin-type gold deposits have common and special features (Wells and Mullens, 1973; Romberger, 1986; Cathelineau et al., 1989; Bakken et al., 1989; Cook and Chryssoulis, 1990).

In hydrothermal ore-forming solutions, the Au(HS)₂⁻

and Au₂S₂⁻ species are the most stable known inorganic complexes of Au⁺ (Seward, 1989). Other species may also exist, such as AuS⁻ (Chen, 1987; Qin, 1987). In hydrothermal solutions containing appreciable As, a certain proportion of S may be complexed with As, and complexes consisting of Au, S, and As, such as Au(S,As)₂⁻, may form. With changes in oxidizing and reducing conditions, temperature, pressure, or pH in the mineralizing environment, the Au complex may decompose leading to Au deposition. When Fe²⁺ and As are present in solution, the decomposition of Au complexes may take place as follows:



Therefore, in various kinds of gold deposits, pyrite is commonly the most important Au-bearing mineral; Au concentration in pyrite is correlated very closely with As concentration; Au usually occurs as micrometer or ultramicroscopic (submicrometer) native gold inclusions.

Knowledge of the special mode of occurrence and distribution characteristics of invisible Au in such ores is useful to metallurgical process design of oxidizing-roasting, chloridizing, and cyanide leaching. In this case, sufficient oxidization and leaching of the pyrite surface layer will produce satisfactory Au recovery.

ACKNOWLEDGMENTS

This work was supported by the Chinese Academy of Geological Sciences. I wish to thank my colleagues, G. Li, L. Bian, W. Lu, Z. Gong, S. Diao, and M. Liu, for giving valuable assistance and suggestions.

REFERENCES CITED

- Bakken, B.M., Hochella, M.F., Marshall, A.F., and Turner, A.M. (1989) High-resolution microscopy of gold in unoxidized ore from the Carlin mine, Nevada. *Economic Geology*, 84, 171-179.
- Boyle, R.W. (1979) The geochemistry of gold and its deposits. *Geological Survey of Canada Bulletin*, 280.
- Cabri, L.J., Chryssoulis, S.L., de Villiers, J.P.R., Laflamme, J.H.G., and Buseck, P.R. (1989) The nature of "invisible" gold in arsenopyrite. *Canadian Mineralogist*, 27, 353-362.
- Cathelineau, M., Boiron, M.C., Holliger, P., Marion, P., and Denis, M. (1989) Gold in arsenopyrite: Crystal chemistry, location and state, physical and chemical conditions of deposition. *Economic Geology*, Monograph 6, 328-341.
- Chen, S. (1987) Geochemistry and mineralization of gold. *Journal of Chengdu College of Geology*, 16, 8-17 (in Chinese).

- Cook, N.J., and Chryssoulis, S.L. (1990) Concentrations of "invisible gold" in the common sulfides. *Canadian Mineralogist*, 28, 1-16.
- Cox, M.G.C. (1983) Experimental determination of X-ray intensities. In V.D. Scott and G. Love, Eds., *Quantitative electron-probe microanalysis*, p. 125-146. Ellis Horwood Ltd., Chichester, England.
- Qin, L. (1987) Principle of transport and deposition of gold. *Science and Technology for Gold*, 2, 62-64 (in Chinese).
- Romberger, S.B. (1986) Disseminated gold deposits. *Geoscience Canada*, 13, 23-31.
- Seward, T.M. (1989) The hydrothermal chemistry of gold and its implications for ore formation: Boiling and conductive cooling as examples. *Economic Geology, Monograph 6*, 398-404.
- Song, D., and Diao, S. (1989) Occurrence and process characteristics of the disseminated gold ore from Southwestern Guizhou and its mineral processing tests. Main types of gold deposits and their mineralization conditions in China, p. 175-203. Geology Press, Beijing.
- Toya, T., and Kato, A. (1983) Practical techniques for microprobe analysis. JEOL Training Center, Tokyo.
- Webster, J.G. (1986) The solubility of gold and silver in the system Au-Ag-S-O₂-H₂O at 25 °C and 1 atm. *Geochimica et Cosmochimica Acta*, 50, 1837-1845.
- Wells, J.D., and Mullens, T.E. (1973) Gold-bearing arsenian pyrite determined by microprobe analysis, Cortez and Carlin gold mines, Nevada. *Economic Geology*, 68, 187-201.
- Zhang, Z., Yang, S., and Yi, W. (1987) Study on submicron gold and lattice gold in some minerals. *Proceedings of the Fourth National Conference on Process Mineralogy*, 60-63 (in Chinese).
- Ziebold, T.O. (1967) Precision and sensitivity in electron microprobe analysis. *Analytical Chemistry*, 39, 858-861.

MANUSCRIPT RECEIVED NOVEMBER 17, 1989

MANUSCRIPT ACCEPTED JUNE 26, 1991